Computers & Geosciences 90 (2016) 179–188

Contents lists available at ScienceDirect

Computers & Geosciences

journal homepage: www.elsevier.com/locate/cageo

Case study

Matched filtering method for separating magnetic anomaly using fractal model

Guoxiong Chen [a,b,*], Qiuming Cheng [a,b,*], Henglei Zhang [c]

[a] State Key Laboratory of Geological Processes and Mineral Resources, China University of Geosciences, Wuhan 430074, Beijing 100083, China
[b] Department of Earth and Space Science and Engineering, York University, Toronto, Canada M3J 1P3
[c] Institution of Geophysics and Geomatics, China University of Geosciences, Wuhan 430074, China

ARTICLE INFO

Article history:
Received 16 October 2015
Received in revised form
7 December 2015
Accepted 19 February 2016
Available online 21 February 2016

Keywords:
Fractal/multifractal
Spectral analysis
Magnetic field separation
Matched filtering

ABSTRACT

Fractal/scaling distribution of magnetization in the crust has found with growing body of evidences from spectral analysis of borehole susceptibility logs and magnetic field data, and fractal properties of magnetic sources have already been considered in processing magnetic data such as the Spector and Grant method for depth determination. In this study, the fractal-based matched filtering method is presented for separating magnetic anomalies caused by fractal sources. We argue the benefits of considering fractal natures of source distribution for data processing in magnetic exploration: the first is that the depth determination can be improved by using multiscaling model to interpret the magnetic data power spectrum; the second is that the matched filtering can be reconstructed by employing the difference in scaling exponent together with the corrected depth and amplitude estimates. In the application of synthetic data obtained from fractal modeling and real aeromagnetic data from the Qikou district of China, the proposed fractal-based matched filtering method obtains more reliable depth estimations as well as improved separation between local anomalies (caused by volcanic rocks) and regional field (crystalline basement) in comparison with the conventional matched filtering method.

1. Introduction

The concept of fractal geometry is introduced by Mandelbrot (1967) to describe, model and analyze the complex phenomenon or process manifesting self-similarity or scale invariance. The past 40 years have seen the extension of fractal concept from geometric sets to multiscaling fields, which significantly increased its applicability (Mandelbrot, 1989; Cheng, 2007; Lovejoy and Schertzer, 2007; Chandrasekhar et al., 2013). A wide range of geofields have been discussed in various power-law scaling or fractal terms, such as radial-density of mineral deposits (Carlson, 1991), density-area of geochemical concentrations (Cheng et al., 1994), magnitude-frequency of earthquakes (Turcotte, 1997) and spectrum-frequency of topography (Gagnon et al., 2006) and geochemical landscapes (Chen et al., 2016), to name but few examples. Such scaling behaviors may represent the end products of numerous independent or nonlinear geo-processes in the lithosphere (Cheng, 2007; Lovejoy and Schertzer, 2007). In last two decades, growing body of evidences from borehole susceptibility logs and magnetic surveys showed that the distribution of crustal magnetization exhibits statistical self-similarity which depicts a power-law dependence of power density spectrum on frequency, the so-called scaling ($1/f^{\beta}$) noise (e.g., Pilkington and Todoeschuck, 1993; Maus and Dimri, 1994; Lovejoy and Schertzer, 2007; Bansal and Dimri, 2014). The scaling exponent (β) measures the correlation of adjacent values within the series. $\beta<0$ indicates a anti-correlated series; $\beta=0$ indicates a completely uncorrelated series (e.g., white noise); $\beta>0$ indicates a correlated series; the series becomes more correlated when β becomes more positive.

In magnetic exploration, the more commonly used assumption in data interpretation is homogeneous source, certainly, standing in contrast to its complex forms observed from well logs. From a inhomogeneous distribution point of view, a random uncorrelated (statistical) model was first used to model magnetization distribution and to interpret magnetic data using the spectral methods (Naidu, 1968; Spector and Grant, 1970). Subsequently, with the fractal nature of sources becoming evident, numerous efforts have been made with an incentive of using fractal concept to facilitate the interpretation of magnetic data. These applications include the kriging interpolation using a fractal covariance model (Pilkington et al., 1994), the inversion for fractal magnetic source distributions (Maus and Dimri, 1995), the Curie depth estimation using scaling spectral analysis (Maus et al., 1997; Ravat et al., 2007;

* Corresponding authors at: State Key Laboratory of Geological Processes and Mineral Resources, China University of Geosciences, Wuhan 430074, China.
E-mail addresses: chengxhg@163.com (G. Chen), qiuming@yorku.ca (Q. Cheng), sky0610@163.com (H. Zhang).

http://dx.doi.org/10.1016/j.cageo.2016.02.015
0098-3004/

Bouligand et al., 2009; Bansal et al., 2011; Bansal et al., 2013), the model-based filtering method (Pilkington and Cowan, 2006) and grid preparation using scaling noise (Pilkington and Keating, 2012). Specifically, fractal model helps to interpret the power spectrum of magnetic data by considering a frequency power-law (scaling) decay besides the depth-dependence exponential decay, and it conducts and improves the depth determination of ensemble source by employing a scaling exponent (β) to correct this power-law decay before applying the Spector and Grant (1970) method.

In this study, we are devoted to use the fractal/multifractal model to facilitate the magnetic field separation of using matched filtering (MF) method. The MF was proposed by Syberg (1972), mainly employing the separation of layers and amplitude ratio to construct the filtering transfer function. However, the conventional MF method is based on the random uncorrelated model, which ignored the fractal/multifractal nature of sources. With this in mind, the proposed fractal-based MF method is centered on two aspects for improving the transfer function: the first is to correct the estimations of depth and amplitude by using scaling spectral analysis. The second is to employ the difference in scaling exponent resulting from fractal/multifractal sources, which usually show different statistical self-similarities in term of inhomogeneous scaling exponent ranging between 1.5 and 5.0 (Bouligand et al., 2009; Pilkington and Keating, 2012). Finally, the fractal-based MF method discussed in this paper is tested using synthetic data generated by fractal modeling and real aeromagnetic data from the Qikou district of China. In this study, we assume that magnetic anomalies are purely caused by induced magnetization without the effects of remanent magnetization.

2. Methodology

2.1. Fractal/scaling nature of sources

Fractals are natural consequence of self-similarity/self-affinity associated with scale-invariance, which refers to the property of a system that does not change by changing scales. This property, in general, can be identified by a power-law relation between a measure $M(\delta)$ and the measuring unit δ, $M(\delta) \propto \delta^{E-D}$, where $\propto$ stands for proportionally. E, D and $E-D$ represent topological dimension, fractal dimension and fractal codimension (scaling exponent), respectively. As mentioned previously, numerous power-law type functions have been used to describe the fractal natures in geosciences. Perhaps the most popular and simplest power-law model to describe fractal geofields (e.g., topography, geochemical landscapes, rains and clouds, etc) is the scaling noise. Recent studies have shown many evidences to support the fractal or at least scaling nature of magnetization distributions by using spectral analysis (e.g., Leonardi and Kümpel, 1996; Zhou and Thybo, 1998; Bansal et al., 2010, etc.), depicting that the power density spectrum (ϕ_m) of magnetization variables has a power-law dependence on the wavenumber (k)

$$\phi_m(k) \propto k^{-\beta_m}. \tag{1}$$

The scaling exponent β_m, as indicator of persistence or type of correlation, could quantify the spatial statistic property of magnetization distributed within the crust. Using a stochastic fractal distribution of 3D magnetization with an isotropic scaling exponent (β_m), Pilkington and Todoeschuck (1993) deduced that the power spectrum (S) of the resulting magnetic field can be written as

$$S(u, v, z) = \frac{8}{\pi}\frac{(-\beta_m - 1)!!}{(-\beta_m)!!}e^{-2kz}k^{-\beta_m+1}, \tag{2}$$

where u and v are the horizontal wavenumber, $k = \sqrt{u^2 + v^2}$ is the radial wavenumber, !! is the double factorial and z is the depth to the top of source distribution. Above model suggests that a fractal magnetic source with β_m could produce fractal magnetic field (at the top of source, i.e. $z=0$) whose power spectrum possesses frequency scaling decay with scaling exponent $\beta_f=\beta_m-1$.

A review of publish data conducted by Bouligand et al. (2009) showed a wide range of β_m estimates between 1.5 and 5.0 for 3D crustal magnetization, based on observation scale from 1 m to 1000 km. Also, their observations suggest that the range of β_m-*value* differs significantly among igneous ($3.1 \le \beta_m \le 5.0$), metamorphic ($2.4 \le \beta_m \le 4.0$) and sedimentary ($1.5 \le \beta_m \le 3.3$) unit/province. In general, the β_m-*value* depends on heterogeneity within the lithological units (Bansal et al., 2010), and measures the composition and balance of stochastic and deterministic components (Wu et al., 1994). For instance, sedimentary provinces generally show smaller β_m-*value* due to the uncorrelated distributions of magnetizations where stochastic components (e.g., heterogeneity and measurement errors) play a leading role, while igneous provinces exhibit bigger β_m-*value* due to the correlated distribution of magnetizations where deterministic components (e.g., lithological units and regional trend) play a leading role. These facts seem to suggest that crustal magnetizations scale with multiple scaling behaviors, the so-called multifractal/multiscaling. Multifractal is a type of fractal in contrast to the monofractal that shows a homogeneous scaling rule across scales, and the multifractal natures of crustal magnetization have already been reported and argued in numerous literatures (e.g., Fedi, 2003; Lovejoy and Schertzer, 2007; Gettings, 2012).

2.2. Matched filtering method using fractal model

Regional–residual separation is a common issue in the interpretation of magnetic data. The regional usually implies deep-sources effects while residual/local implies shallow effects. Many filtering methods have been designed to implement regional–residual separation, such as matched filtering (MF), wavelet decomposition (Fedi and Quarta, 1998) and empirical model decomposition (Huang et al., 2010), etc. The advantage of MF over other kind of filters is that the MF has geologically constrained benefits including a class of geological models and its depth determination, whereas other methods do not have. Based on a stochastic uncorrelated source distribution, the resulting magnetic field power spectrum is simply characterized by a depth-dependent exponential decay; therefore, the MF method was designed for separating regional–residual components by using the natural break in the spectrum slope (Spector and Grant, 1970; Syberg, 1972). For a simplest case of two ensemble sources, we have a deep-seated source and a shallow source with average depth to the top of the body H and h, respectively. The power spectrum of magnetic field caused by deep (S_1) and shallow (S_2) sources can be written as

$$S_1(k) = A^2e^{-2kH}, \tag{3}$$

$$S_2(k) = a^2e^{-2kh}. \tag{4}$$

where A^2 and a^2 are the intercept (amplitude) value of power spectrum.

However, above simplified spectrum model ignored the additional frequency power-law (scaling) decay evidenced in real power spectrum of magnetic data (Pilkington et al., 1994; Maus

and Dimri, 1995; Bansal and Dimri, 2014). Although the scaling distribution is only but one that lead to this specific form of power spectrum and scaling magnetic field cannot guarantee the fractal nature of sources because of the non-uniqueness of potential fields, a scaling correlated model is more realistic to interpret the spectra than the earlier assumption of random uncorrelated model in Spector and Grant method (Fedi et al., 1997). According to Eq. (2), the fractal distribution of sources would produce the magnetic field whose power spectrum is dominated by both a depth-dependent exponential and a frequency scaling decay. Therefore, (Eqs. (3) and 4) can be rewritten as

$$S_1(k) = A^2 k^{-\beta_1} e^{-2kH}, \tag{5}$$

$$S_2(k) = a^2 k^{-\beta_2} e^{-2kh}, \tag{6}$$

where β_1 and β_2 are the scaling exponent of magnetic field, resulting from the deep and shallow sources with fractal behaviors, respectively.

Then the power spectrum (E) of combined magnetic anomalies is given by

$$E(k) \approx (Ak^{-\beta_1/2} e^{-kH} + ak^{-\beta_2/2} e^{-kh})^2$$

$$= \left[Ak^{-\beta_1/2} e^{-kH} (1 + (a/A)\, k^{\Delta\beta/2} e^{k(H-h)}) \right]^2, \tag{7}$$

where $\Delta\beta = \beta_1 - \beta_2$ indicates the difference in scaling exponent between deep and shallow sources. According to the general definition of MF transfer function in Syberg (1972), the new transfer function of fractal-based MF can be obtained as

$$W(k) = \left[1 + (a/A)\, k^{\Delta\beta/2} e^{k(H-h)} \right]^{-1}, \tag{8}$$

for separating out the regional components from the mixed magnetic field.

The transfer function of fractal-based MF achieves improvements in two aspects compared with that of (conventional) random-based MF. Firstly, the depth estimations (H, h) of deep and shallow sources are corrected by using multiple scaling exponent in light of multiscaling source distributions; accordingly, the amplitude ratio (a/A) also is corrected. The correction of depth determination using fractal parameter has already been demonstrated in many literatures (e.g., Fedi et al., 1997; Ravat et al., 2007; Bouligand et al., 2009; Bansal et al., 2011), but a single scaling exponent (indicating monofractal) is often used to interpret the overall spectrum, which should not be appropriate since the practical magnetic sources actually show multiscaling properties (Lovejoy et al., 2001; Pecknold et al., 2001; Gettings, 2012). Magnetic field data arising from the superposition of ensemble sources with different depths and multifractal properties shows a power spectrum which may find with two or more combined regimes of scaling and exponential model. Therefore, the fractal-based MF method uses a more realistic model for interpreting the magnetic data including depth estimation and field separation. Secondly, the fractal-based MF transfer function in Eq. (8) employs the multifractal nature of source distribution. It is known that in conventional MF whether a good separation is possible is determined by the separation between layers ($H-h$) and amplitude ratio (a/A). For an extreme case of $H-h=0$ and $a/A=1$, the conventional MF cannot work due to the constant filter response (viz. $W=0.5$). However, the fractal-based MF considers a new physical (fractal) property, namely scaling-difference ($\Delta\beta/2$) for regional–residual separation, and the resulting filter response is capable of separating anomaly even if the deep and shallow sources only possess scaling difference with same depth and amplitude.

Several studies suggested that a simultaneous estimation of scaling exponent and depth is difficult to obtain from the power spectrum curve by using inversion method (e.g., Bouligand et al., 2009; Bansal and Dimri, 2014), and the algorithm would become complicated for such estimations of multiple sources. Nonetheless, the independent estimation of the average depth can be obtained from seismic interpretation and other potential field methods (e.g., Euler deconvolution and analytic signal), also the scaling exponent can be estimated from borehole susceptibility logs. As suggested by Bouligand et al. (2009), once one of the two parameters is specified then another becomes straightforward. In addition, Fedi et al. (1997) proposed that a "blocky" distribution of magnetization (e.g., crystalline basement) could produce a inherent scaling decay rate of $\beta \approx 3$ which is often found in published data, and the reported β estimates in Bouligand et al. (2009) also imply that $|\Delta\beta/2|$ has a small range between 0 and 1.75. These facts provide priori constraints for constructing the fractal-based MF. In the subsequent sections, the model test and real case study are undertaken to validate the performance of fractal-based MF method requiring the independent estimate of scaling exponent or source depth.

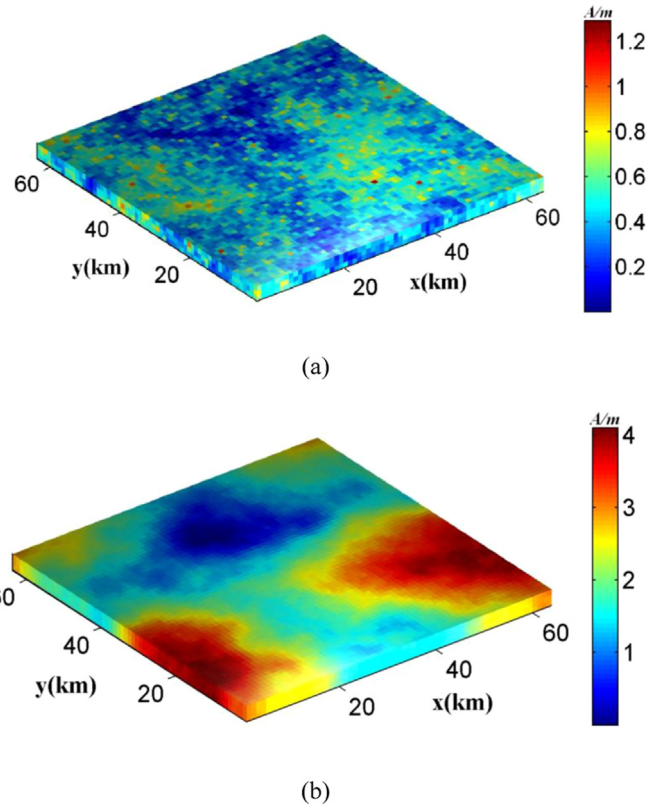

Fig. 1. Synthetic 3D magnetic sources consisting of $64 \times 64 \times 4$ blocks of 1 km size with fractal magnetization distribution. (a) Upper layer, the depth to top surface (h) is 1 km, magnetization (M) is 0.5 A/m, and scaling exponent $\beta_m=2$. (b) Lower layer, $H=10$ km, $M=2$ A/m, and $\beta_m=4$.

3. Synthetic data

Fractal modeling presented in Pilkington and Todoeschuck (1993) is used to simulate 3D fractal distribution of magnetization and generate synthetic magnetic anomalies. Firstly, we generate white noise of lognormal distribution in a 3D block. Then the 3D magnetization values are Fourier transformed and multiplied by $(u^2 + v^2 + w^2)^{-\beta_m/4}$, where β_m is the required scaling exponent and w is the wavenumber in z-direction. Subsequently, inverse Fourier transformation gives the desired fractal magnetization model. The

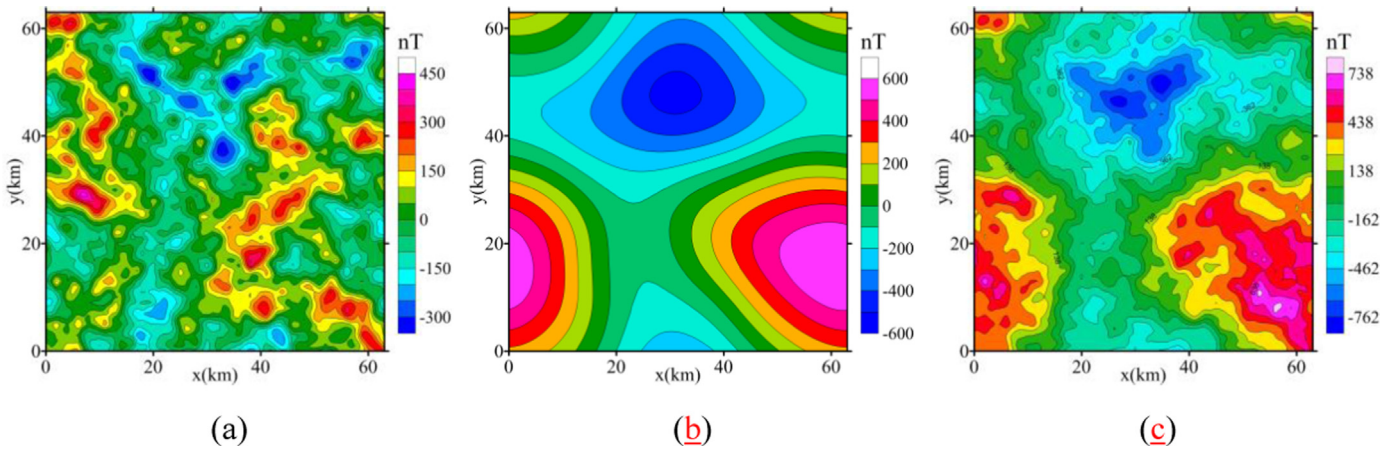

Fig. 2. Synthetic magnetic anomalies. (a) Upper layer anomaly, (b) lower layer anomaly and (c) combined anomaly.

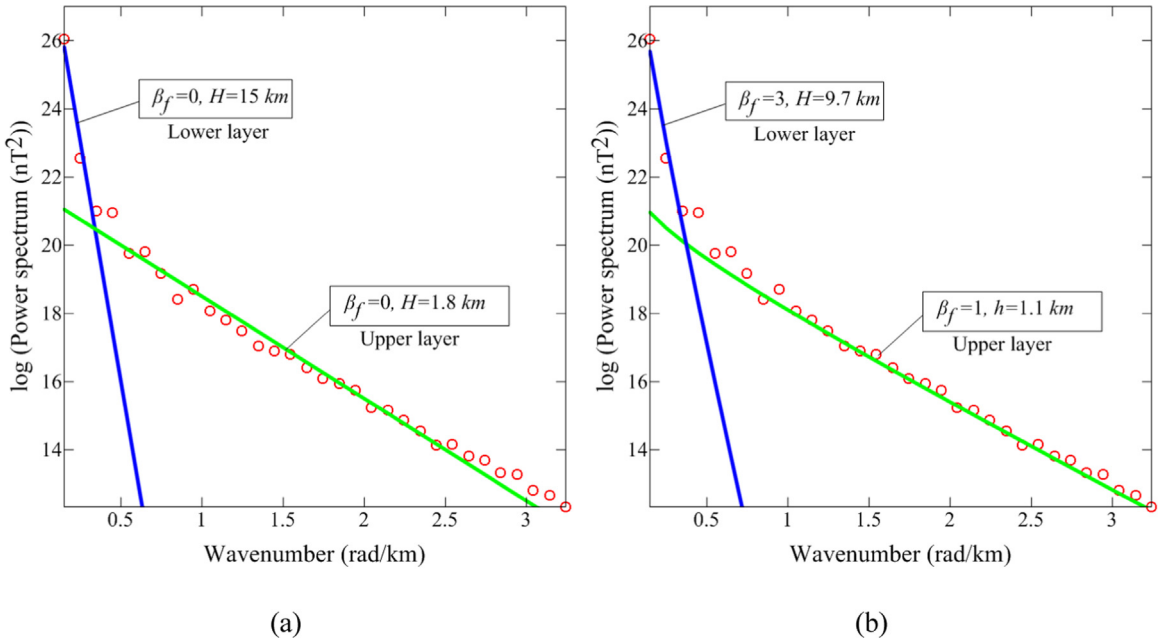

Fig. 3. Radially averaged power spectrum of the combined magnetic data. (a) Model fits of spectrum data using an exponential decay, the so-called Spector and Grant model. (b) Model fits of spectrum using fractal model integrating scaling and exponential decays.

power spectrum of the product is therefore proportional to $(u^2 + v^2 + w^2)^{-\beta_m/2}$. Finally, this fractal distribution model is used to generate the magnetic field, which possesses a frequency-scaling decay ($k^{-\beta_m+1}$) in its power spectrum.

For a common case of regional–residual components separation, we simulate a two-layer model with fractal magnetization distribution, representing sedimentary sources (with heterogeneities) overlaying a crystalline basement. From the previous discussion, we assume that crystalline layer has a larger scaling exponent than sedimentary layer. Specifically, the upper layer (Fig. 1a) extends from 1 to 4 km depth and has an average magnetization M=0.5 A/m and a scaling exponent β_m=2. The lower layer (Fig. 1b) extends from 10 to 14 km with M=2 A/m and β_m=4. Fig. 2a and b shows the magnetic field contributions from the upper and lower layers, respectively. Fig. 2c shows the combined magnetic anomalies produced by this constructed two-layer model. From the spectral analysis of synthetic anomalies (Fig. 2c), it is observed that the power spectrum (Fig. 3a) produces two distinct segments. Lower wavenumber portion implies the lower layer while intermediate-higher wavenumbers implies the upper layer.

The break in the spectrum segments indicates that MF method is suitable for separating the mixed anomalies between lower and upper sources. Firstly, the model test is to validate the improvement of depth determination of spectrum method using fractal model over uncorrelated model. The top depths of lower and upper layers are estimated as H=15 km and h=1.8 km (Fig. 3a) using the exponential decay to fit spectrum data based on uncorrelated model, while these depth values are estimated as H=9.7 km and h=1.1 km (Fig. 3b) by using the fractal model that integrates exponential and scaling decays to fit spectrum data. It suggests that the fractal model obtaines improved depth estimation compared with uncorrelated model. Note that we specified β_f=1 and 3 in (Eqs. (5) and 6), respectively, to fit the spectrum data of lower and higher wavenumber portions using the least square regression, and the half of the slope is the estimation of depth. Additionally, the amplitude value was obtained as $a^2=e^{20}$ and $A^2=e^{22}$ for fractal models and $a^2=e^{21}$ and $A^2=e^{27}$ for uncorrelated models.

Secondly, this model test is to address the comparison among conventional, monofractal-based and multifractal-based MF method. Note that the monofractal model means no difference in scaling exponent, viz., $\Delta\beta$=0 in Eq. (8). The parameters (H, h, a/A

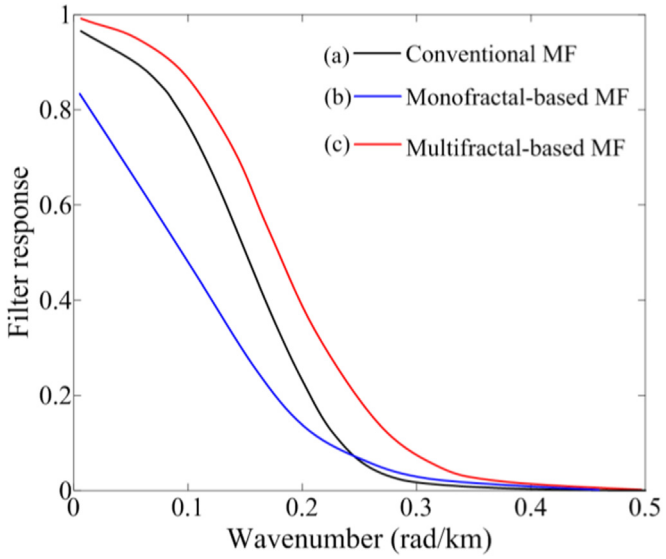

Fig. 4. Transfer function of MF based on random (β=0), monofractal ($\Delta\beta$=0) and multifractal ($\Delta\beta$=2) source distribution.

or $\Delta\beta$) are then used to construct the MF transfer function for separating magnetic anomalies (Fig. 2c). Fig. 4a shows the filter response of conventional MF, where *H*, *h*, and *a*/*A* are obtained using random uncorrelated model. Fig. 4b and c shows the filter response of monofractal-based ($\Delta\beta$=0) and multifractal-based ($\Delta\beta$=2) MF, respectively, where *H*, *h*, and *a*/*A* are obtained using fractal distribution in Fig. 3b. Then three groups of residual–regional (upper–lower) separations are obtained in Fig. 5a–b, c–d and e–f using the random-, monofractal- and multifractal-based MF, respectively. Cursory comparison of patterns between Figs. 2 and 5 suggests that multifractal-based MF obtains better separation of the two different layer responses than that of random – and monofractal – based MF, since Fig. 5a and c contains long wavelengths that may be basement anomalies whereas Fig. 5e does not. It also can be observed from the difference maps (Fig. 6) of Fig. 5e–a and e–c showing distinct patterns of basement response. Subsequently, the *rms* errors between the real contribution of upper layer and separated residual component are calculated as 55, 165 and 46 nT, respectively, corresponding to Fig. 5a, c and e, and the correlation coefficients are 0.89, 0.76 and 0.93. This result suggests that the multifractal-based MF obtained the best field separation between upper and lower layers. Note that the conventional MF outperforms monofractal-based MF for residual–regional separation. In fact, in case of mono-fractal and conventional MF the value of $\Delta\beta$ becomes zero and response curve of filter is controlled mainly by depth separation and amplitude ratio. The depth values will be significantly lower in case of monofractal than the conventional mainly for lower wavenumber portion (see in Fig. 3). Therefore, filter response became worse as compared with conventional MF since the conventional overestimated the depth separation value. All in all, the multifractal-based MF improves the separation of magnetic field on one hand, on the other hand obtaines more reliable depth estimation of sources.

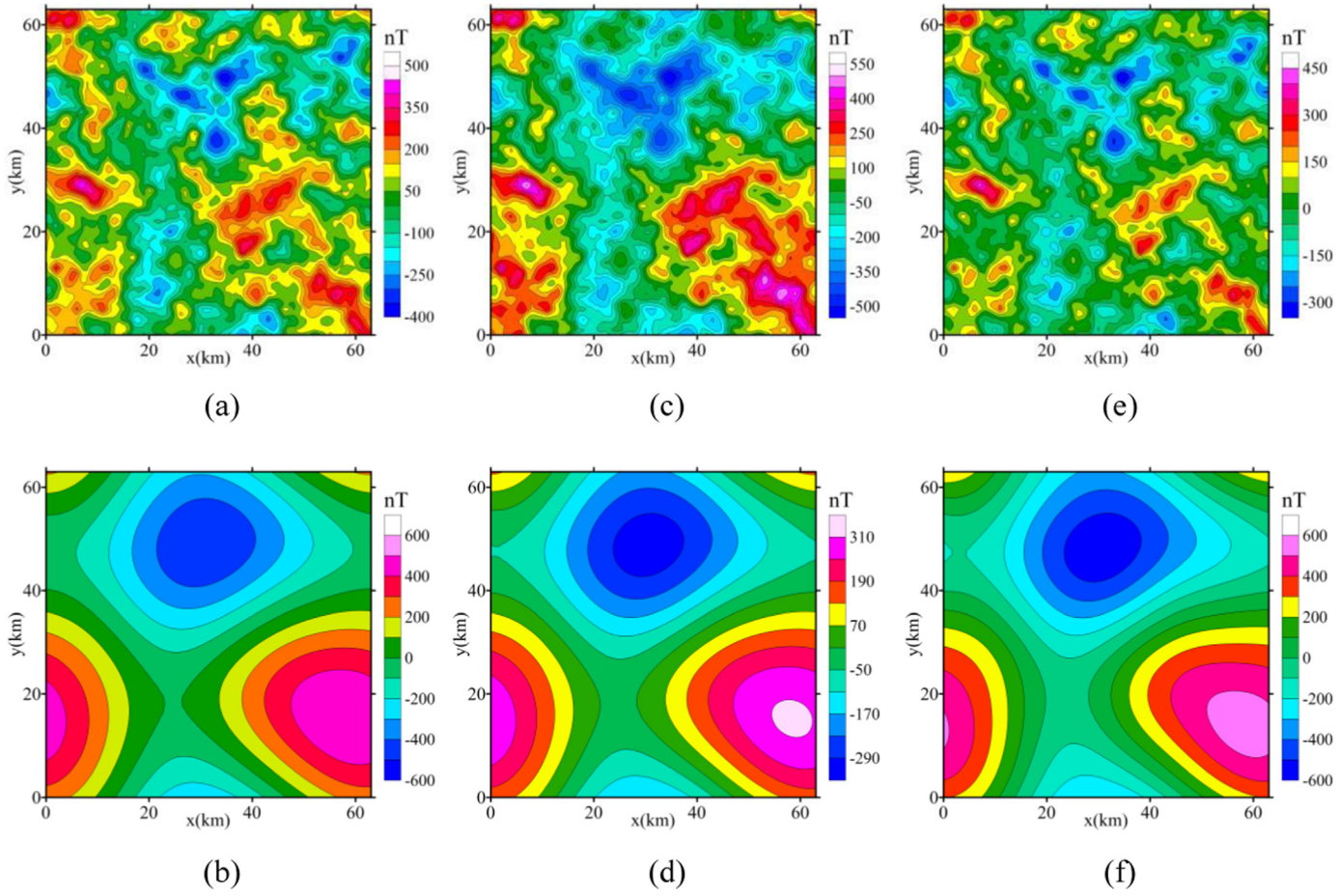

Fig. 5. Field separations between two layers. (a, b) Upper and lower components, respectively, obtained from conventional MF method. (c, d) obtained from monofractal-based MF; (e, f) obtained from multifractal-based MF.

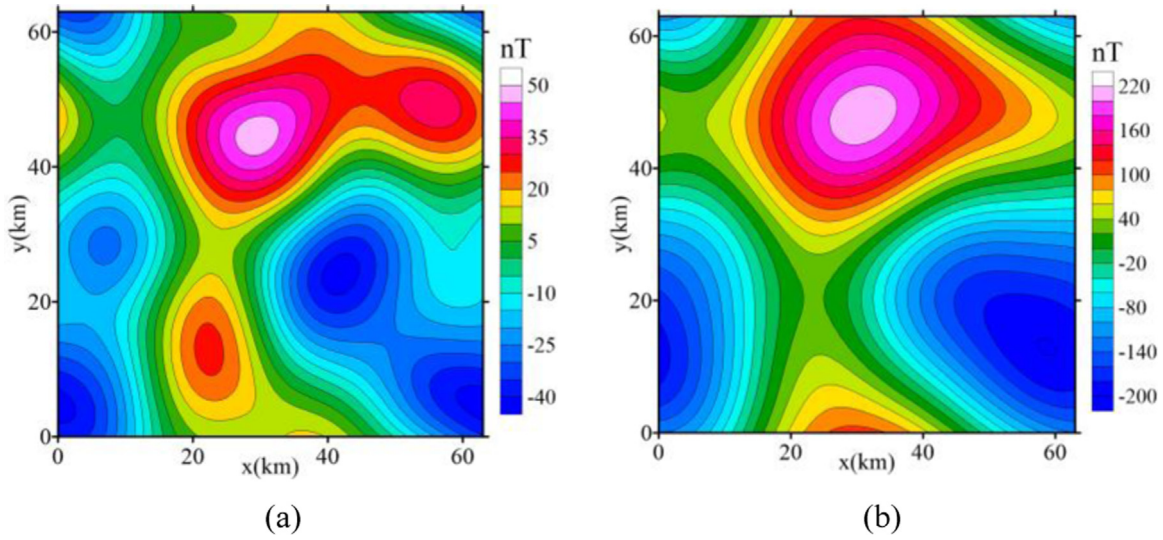

Fig. 6. Difference maps of (a) Fig. 5e subtracting Fig. 5a and (b) Fig. 5e subtracting Fig. 5c.

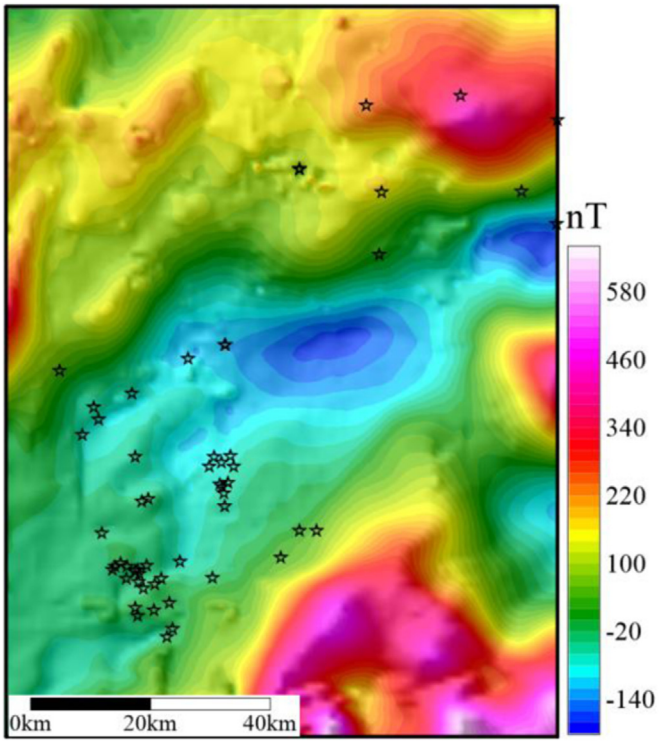

Fig. 7. Aeromagnetic anomaly reduced to the pole in Dagang district. Pentagrams indicate the locations of drill holes that found volcanic rocks.

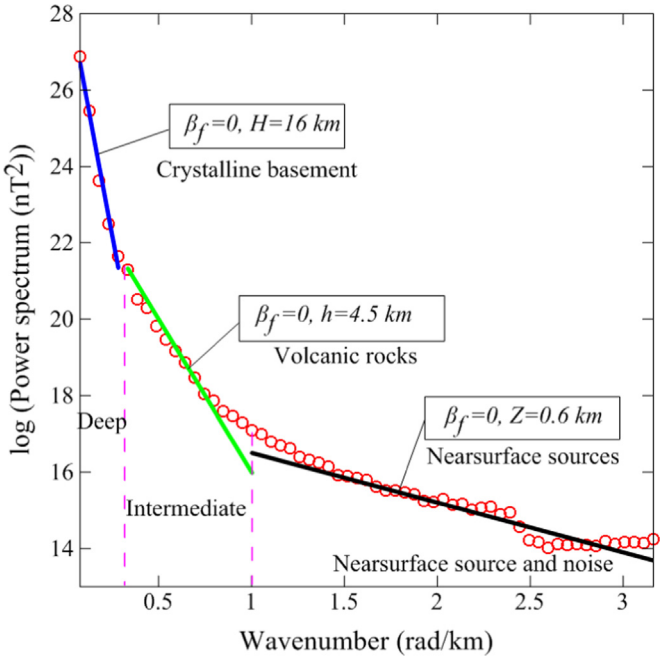

Fig. 8. Radially averaged power spectrum of RTP aeromagnetic field data. Spector and Grant model (lines) was used to fit the power spectrum data (dots), then to estimate the depth and amplitude values to construct the conventional MF transfer function.

4. Application to real case

4.1. Geological setting

The Qikou main sag is located in the northern central part of the Huanghua depression of the Bohai Bay basin in eastern China. To date, seven volcanic reservoirs and two oilfields producing ten million tons of oil per year have been identified in the Qikou depression. Cenozoic volcanic rocks (e.g. basalts, andesites, diabases, and volcanic tuffs) occur extensively throughout the Qikou depression and primarily in the sedimentary strata of Shahejie, Dongying, and Guantao formations. The statistic on the magnetic susceptibilities of rocks from Huanghua depression and adjacent area have been conducted in Hao et al. (2008) and Yang et al. (2010). Most volcanic rocks exhibit higher magnetic susceptibilities that range between 200×10^{-5} SI and 4000×10^{-5} SI, while the susceptibilities of the Mesozoic and Cenozoic basin sediments (mudstone and sandstone) range between 0×10^{-5} SI and 83×10^{-5} SI. The crystalline basement in this area is composed of gneisses and amphibolites, which have strong magnetic susceptibility bigger than 3500×10^{-5} SI, and its top surface corresponds to the interface between Paleozoic and Archean stratums. Volcanic rocks and crystalline basement are the main causative sources producing magnetic anomalies. The drill holes have evidenced that the volcanic rocks in Qikou depression are primarily buried at depths between 1.9 km and 3.5 km (Wu et al., 2010; Yang et al., 2010), and seismic reflection data suggestes that the average depth

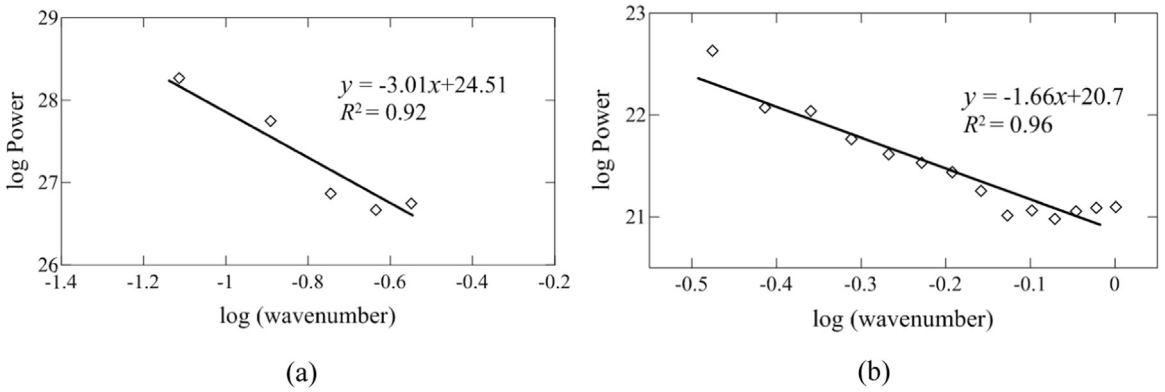

Fig. 9. Estimation of *β-value* for crystalline basement (a) and volcanic layer (b). Dots represent the spectrum subtracting the depth-dependent exponential decay and lines represent model fits using a power-law relation. *β-value* is estimated from the slope of spectrum against wavenumber in log-log scale.

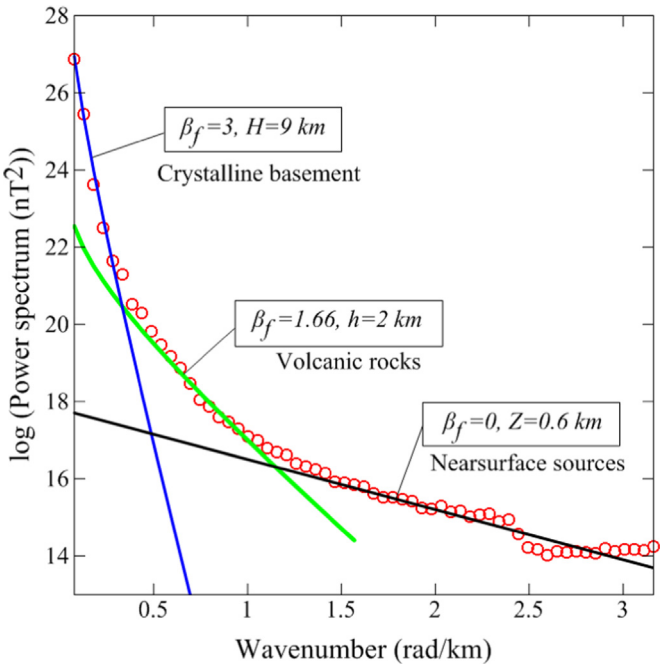

Fig. 10. Model fits of radially averaged power spectrum using the combined model of power-law and exponential decays, considering fractals nature of sources.

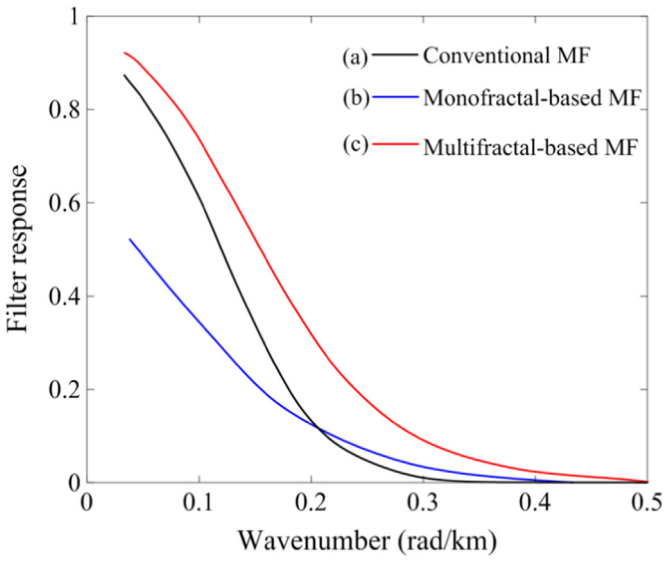

Fig. 11. Transfer function of MF based on random, monofractal ($\Delta\beta=0$) and multifractal ($\Delta\beta=1.4$) source distribution.

to the top of crystalline basement (Archean stratum) is around 9 km (Hao et al., 2008).

4.2. Data processing result

Fig. 7 shows the aeromagnetic field reduced to the pole (RTP) in the Qikou district. The regional magnetic inclination and declination are 56° and −6°, respectively. Long wavelength portion of the observed field are produced by the crystalline basement; medium–short wavelength portion anomalies may mainly arise from volcanic rocks. From the locations of drill holes (Fig. 7) intersecting volcanic, no significant anomaly patterns can be observed due to the deep buried volcanic rocks as well as the interference of strong background field. Therefore, identifying the weak anomalies of volcanic rocks would help delineate the potential distribution of volcanic oil reservoirs. Here, the MF method is undertaken to separate magnetic anomalies between volcanic rocks and crystalline basement, with intention to test the performance of the proposed fractal-based MF.

The radially averaged power spectrum of RTP aeromagnetic data is first calculated (Fig. 8), and it presents three segments that may be interpreted as a three-ensemble case indicating crystalline basement, volcanic rocks and near-surface sources (noise). Here, we regard the volcanic intrusions distributed within the sedimentary strata as an ensemble source (viz. magnetized layer) with depth ranging from 1.9 km to 3.5 km. To construct the MF transfer function, we need to specify the parameters H, h, a/A or $\Delta\beta$. Using the conventional MF, the depth values of three ensemble sources are estimated as 16 km, 4.5 km and 0.6 km. From the observed values from drill holes and seismic data it is known that the conventional MF overestimated the top depth of volcanic layer and crystalline basement, which may be due to the ignorance of fractal nature of source distribution. The conventional MF transfer function (Fig. 11a) is then constructed using these overestimated parameters, and the aeromagnetic data is decomposed into regional and residual components (Fig. 12a and b). It can be observed that the residual anomalies in volcanic area A (Fig. 12a) are still buried, and in area B it contains obvious long wavelength components indicating the regional field caused by crystalline basement.

To construct the fractal-based MF transfer function, we need to estimate the scaling exponents of sources. A priori knowledge of top–depth of volcanic layer and crystalline basement makes the β estimation become straightforward in this study. After subtracting the exponential decay (e^{-4} and e^{-18} for deep and intermediate portion of spectra, respectively), we can determine the scaling

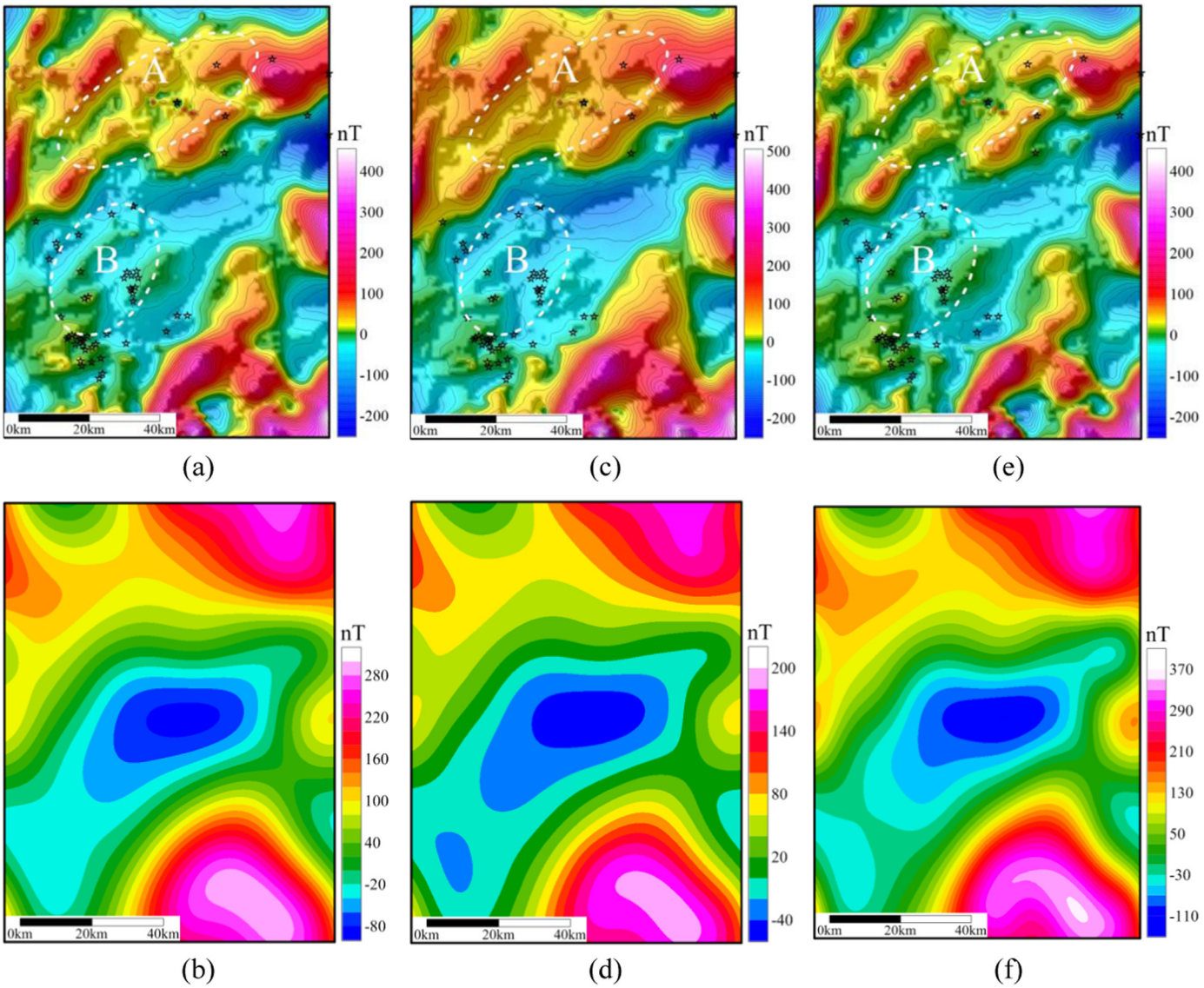

Fig. 12. Field separations between volcanic rocks and crystalline basement. (a, b) residual and regional components, respectively, obtained from conventional MF method. Similarly, (c, d) obtained from monofractal-based MF; (e, f) obtained from multifractal-based MF. Contours of (a), (c) and (e) have same color-bar. (For interpretation of the references to color in this figure legend, the reader is referred to the web version of this article.)

exponent value from the log-log plot of de-exponential spectrum against wavenumber (Fig. 9). The scaling exponents of crystalline basement and volcanic layer are then estimated as $\beta_f \approx 3.0$ and $\beta_f \approx 1.7$ using the slope of de-exponential spectrum in Fig. 9a and b, respectively. It can be observed that the spectrum curve in Fig. 10 is better fitted using the fractal model involving scaling and exponential decays compared with uncorrelated model (Fig. 8). The volcanic layer has smaller scaling exponent due to the intrusions inhomogeneously distributed within the sedimentary strata, while the crystalline basement shows higher scaling exponent ($\beta_f \approx 3.0$) due to the "blocky" distribution of magnetization.

The new parameters (H, h, a/A or $\Delta\beta$) are then used to reconstruct the transfer function for monofractal-based (Fig. 11b) and multifractal-based MF (Fig. 11c). It is observed that monofractal-based MF was failed to separate the anomalies between volcanic layer and crystalline basement (Fig. 12c), whereas the multifractal-based MF obtained a good separation since its residual map (Fig. 12e) shows significant patterns indicating the distribution of volcanic rocks. In comparison with the residual components (Fig. 12a) obtained by conventional MF, the multifractal-based result also shows an improved separation between volcanic layer and crystalline basement. For instance, residual components (Fig. 12e) in volcanic area A present more significant anomalies by multifractal-based MF, and in area B they have less interferences of regional field. Furthermore, the difference maps (Fig. 13) of Fig. 12e–a and e–c suggest that the volcanic anomalies (area A) have been enhanced and basement interferences (area B) have been reduced by multifractal-based MF.

5. Conclusions

Fractal/multifractal nature, as a portrayal of complex source distribution, was considered in the interpretation of magnetic data. Fractal-based matched filtering (MF) method for separating the magnetic field has been presented in this contribution. We used a combined model involving both depth-dependent exponential and frequency-scaling decays to interpret the power spectrum of magnetic data. Multiscaling model helped to improve the depth determination of fractal sources, and the scaling-difference was employed to reconstruct the transfer function of MF. Although the fractal-based MF method requires the independent

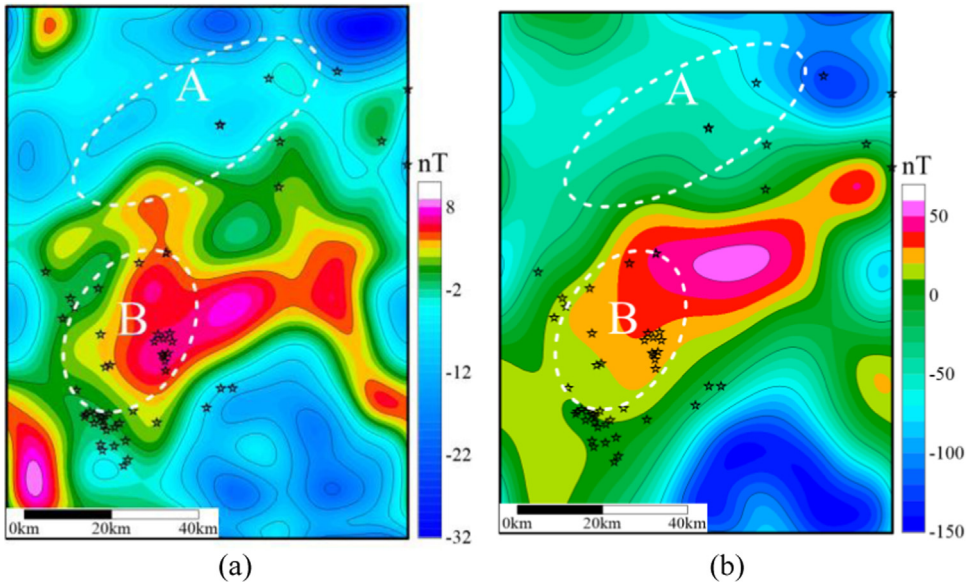

Fig. 13. Difference maps of (a) Fig. 12e subtracting Fig. 12a and (b) Fig. 12e subtracting Fig. 12c.

estimates of source depth or scaling exponent in practical data analysis showing a complicated algorithm, it indeed provides a more realistic model for interpreting the magnetic data compared with the conventional MF using random uncorrelated model. Moreover, both the model test and case study demonstrated that the fractal-based MF obtained more reliable depth estimations as well as improved separation between local anomalies (caused by volcanic rocks) and regional field (crystalline basement).

Acknowledgments

Thanks are due to Dr. Mark Pilkington, Yaoguo Li and Jef Caers for their kindly helps for enhancing this paper. Constructive and thoughtful comments by Prof. Abhey Ram Bansal, Mark Getting and three anonymous reviewers are much appreciated. This work benefits from the National Natural Science Foundation of China (No. 41272362, 41572315 and 41430320), a China Geology Survey project (No. 12120113089000) and a special Student Fund Project (WHS201311).

References

Bansal, A., Anand, S., Rajaram, M., Rao, V., Dimri, V., 2013. Depth to the bottom of magnetic sources (DBMS) from aeromagnetic data of central India using modified centroid method for fractal distribution of sources. Tectonophysics 603, 155–161.
Bansal, A., Dimri, V., 2014. Modelling of magnetic data for scaling geology. Geophys. Prospect. 62, 385–396.
Bansal, A., Gabriel, G., Dimri, V., 2010. Power law distribution of susceptibility and density and its relation to seismic properties: an example from the German Continental Deep Drilling Program (KTB). J. Appl. Geophys. 72, 123–128.
Bansal, A., Gabriel, G., Dimri, V., Krawczyk, C., 2011. Estimation of depth to the bottom of magnetic sources by a modified centroid method for fractal distribution of sources: an application to aeromagnetic data in Germany. Geophysics 76, L11–L22.
Bouligand, C., Glen, J.M., Blakely, R.J., 2009. Mapping Curie temperature depth in the western United States with a fractal model for crustal magnetization. J. Geophys. Res.: Solid Earth (1978–2012) 114.
Carlson, C.A., 1991. Spatial distribution of ore deposits. Geology 19, 111–114.
Chandrasekhar, E., Dimri, V., Gadre, V.M., 2013. Wavelets and Fractals in Earth System Sciences. Taylor & Francis, Abingdon.
Chen, G., Cheng, Q., Zuo, R., 2016. Fractal analysis of geochemical landscapes using scaling noise. J. Geochem. Explor. 161, 62–71.
Cheng, Q., 2007. Multifractal imaging filtering and decomposition methods in space, Fourier frequency, and eigen domains. Nonlinear Process. Geophys. 14, 293–303.
Cheng, Q., Agterberg, F., Ballantyne, S., 1994. The separation of geochemical anomalies from background by fractal methods. J. Geochem. Explor. 51, 109–130.
Fedi, M., 2003. Global and local multiscale analysis of magnetic susceptibility data. Pure Appl. Geophys. 160, 2399–2417.
Fedi, M., Quarta, T., 1998. Wavelet analysis for the regional-residual and local separation of potential field anomalies. Geophys. Prospect. 46, 507–525.
Fedi, M., Quarta, T., De Santis, A., 1997. Inherent power-law behavior of magnetic field power spectra from a Spector and Grant ensemble. Geophysics 62, 1143–1150.
Gagnon, J.-S., Lovejoy, S., Schertzer, D., 2006. Multifractal earth topography. Nonlinear Process. Geophys. 13, 541–570.
Gettings, M., 2012. Multifractal model of magnetic susceptibility distributions in some igneous rocks. Nonlinear Process. Geophys. 19, 635–642.
Hao, T., Xu, Y., Zhou, L., Zhang, L., Jiang, W., Xu, Y., Li, J., Zhao, B., Wang, B., Yuan, S., 2008. Integrated geophysical research on macroscopic distribution of Pre-Cenozoic residual basins—a case in Dagang area. Chin. J. Geophys. 51, 491–502.
Huang, J., Zhao, B., Chen, Y., Zhao, P., 2010. Bidimensional empirical mode decomposition (BEMD) for extraction of gravity anomalies associated with gold mineralization in the Tongshi gold field, Western Shandong Uplifted Block, Eastern China. Comput. Geosci. 36, 987–995.
Leonardi, S., Kümpel, H.-J., 1996. Scaling behaviour of vertical magnetic susceptibility and its fractal characterization: an example from the German Continental Deep Drilling Project (KTB). Geol. Rundsch. 85, 50–57.
Lovejoy, S., Pecknold, S., Schertzer, D., 2001. Stratified multifractal magnetization and surface geomagnetic fields—I. Spectral analysis and modelling. Geophys. J. Int. 145, 112–126.
Lovejoy, S., Schertzer, D., 2007. Scaling and multifractal fields in the solid earth and topography. Nonlinear Process. Geophys. 14, 465–502.
Mandelbrot, B., 1967. How long is the coast of Britain. Science 156, 636–638.
Mandelbrot, B., 1989. Multifractal measures, especially for the geophysicist. Pure Appl. Geophys. 131, 5–42.
Maus, S., Dimri, V., 1994. Scaling properties of potential fields due to scaling sources. Geophys. Res. Lett. 21, 891–894.
Maus, S., Dimri, V., 1995. Potential field power spectrum inversion for scaling geology. J. Geophys. Res.: Solid Earth (1978–2012) 100, 12605–12616.
Maus, S., Gordon, D., Fairhead, D., 1997. Curie-temperature depth estimation using a self-similar magnetization model. Geophys. J. Int. 129, 163–168.
Naidu, P., 1968. Spectrum of the potential field due to randomly distributed sources. Geophysics 33, 337–345.
Pecknold, S., Lovejoy, S., Schertzer, D., 2001. Stratified multifractal magnetization and surface geomagnetic fields—II. Multifractal analysis and simulations. Geophys. J. Int. 145, 127–144.
Pilkington, M., Cowan, D.R., 2006. Model-based separation filtering of magnetic data. Geophysics 71, L17–L23.
Pilkington, M., Gregotski, M., Todoeschuck, J., 1994. Using fractal crustal magnetization models in magnetic interpretation1. Geophys. Prospect. 42, 677–692.
Pilkington, M., Keating, P., 2012. Grid preparation for magnetic and gravity data using fractal fields. Nonlinear Process. Geophys. 19, 291–296.
Pilkington, M., Todoeschuck, J., 1993. Fractal magnetization of continental crust. Geophys. Res. Lett. 20, 627–630.
Ravat, D., Pignatelli, A., Nicolosi, I., Chiappini, M., 2007. A study of spectral methods of estimating the depth to the bottom of magnetic sources from near-surface magnetic anomaly data. Geophys. J. Int. 169, 421–434.

Spector, A., Grant, F., 1970. Statistical models for interpreting aeromagnetic data. Geophysics 35, 293–302.
Syberg, F., 1972. A fourier method for the regional-residual problem of potential field. Geophys. Prospect. 20, 47–75.
Turcotte, D.L., 1997. Fractals and Chaos in Geology and Geophysics. Cambridge University Press, Cambridge.
Wu, R.S., Xu, Z., Li, X.P., 1994. Heterogeneity spectrum and scale-anisotropy in the upper crust revealed by the German Continental Deep-Drilling (KTB) Holes. Geophys. Res. Lett. 21, 911–914.
Wu, X.Y., Liu, T.Y., Su, J.Q., 2010. Gravity and magnetic anomaly characteristics and oil & gas geological significance in middle and north part of the Huanghua Depression. Oil Geophys. Prospect. 45, 140–145.
Yang, Y.S., Li, Y.Y., Liu, T.Y., 2010. Continuous wavelet transform, theoretical aspects and application to aeromagnetic data at the Huanghua Depression, Dagang Oilfield, China. Geophys. Prospect. 58, 669–684.
Zhou, S., Thybo, H., 1998. Power spectra analysis of aeromagnetic data and KTB susceptibility logs, and their implication for fractal behavior of crustal magnetization. Pure Appl. Geophys. 151, 147–159.